

Effects of Concerted Hydrogen Bonding of Distal Histidine on Active Site Structures of Horseradish Peroxidase. Resonance Raman Studies with Asn70 Mutants[†]

Masahiro Mukai,[‡] Shingo Nagano,^{§,⊥} Motomasa Tanaka,[§] Koichiro Ishimori,[§] Isao Morishima,[§] Takashi Ogura,[‡] Yoshihito Watanabe,[‡] and Teizo Kitagawa^{*,‡}

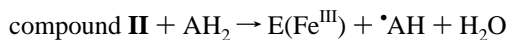
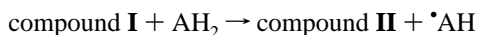
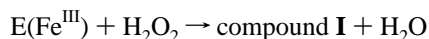
Contribution from the Institute for Molecular Science, Okazaki National Research Institutes, Okazaki 444, Japan, and Division of Molecular Engineering, Graduate School of Engineering, Kyoto University, Kyoto 606-01, Japan

Received July 24, 1996[⊗]

Abstract: Effects of a highly conserved hydrogen bond between the distal histidine (His) and a nearby asparagine residue (Asn) of peroxidases upon the active site structures were investigated using resonance Raman (RR) and EPR spectroscopy. Although there is no crystallographic data for horseradish peroxidase (HRP), Asn70 is deduced to be the hydrogen bond acceptor for HRP. Accordingly, site-directed mutagenesis of Asn70 to Val (N70V) and to Asp (N70D) was carried out with HRP, and their RR spectra were compared with those of native and wild type (WT) enzymes in the resting, reduced, CN-bound ferric and compound **I** states. In the resting state, the six-coordinate high-spin structure is the main component for N70V and N70D mutants, while the five-coordinate high-spin structure is dominant for the native and WT HRP. This was confirmed with EPR spectra. The Fe^{III}–CN stretching ($\nu_{\text{Fe–CN}}$) and bending RR bands of the linear and bent forms were identified using ¹²C¹⁵N and ¹³C¹⁴N isotopes. The $\nu_{\text{Fe–CN}}$ frequency of the linear form is lower for the mutants than for native enzyme, and the spectral patterns of the mutants at pH 7.0 resemble that of the basic form of native HRP. The Fe–histidine stretching bands of reduced HRP exhibit pH dependent frequency shifts, and the midpoint pH values were 7.2, 5.9, and 5.5 for native, N70V, and N70D, respectively. This change is ascribed to the acid–base transition of the distal His. While the Fe^{IV}=O stretching ($\nu_{\text{Fe=O}}$) frequency of compound **I** at pD 7.0 is lower than that at pD 10.0 for native enzyme, the $\nu_{\text{Fe=O}}$ band of the mutants show no pH dependent frequency shifts between pD 7.0 and pD 10.0. However, the H₂O/D₂O frequency change of $\nu_{\text{Fe=O}}$ and the oxygen atom exchange with bulk water suggested the presence of the hydrogen bond between the oxygen ligand of the ferryl-oxo heme and distal His for these mutants at pD 10.0. On the basis of these observations, it is proposed that the hydrogen bond between the N_δ-proton of distal His and Asn70 regulates the pK_a of the N_ε-proton (and thus the reactivity of compound **I** at the distal side) and also affects the Fe–His bond at the proximal side via tertiary structure changes.

Introduction

Horseradish peroxidase (HRP) is a protoheme-containing monomer enzyme which catalyzes the oxidation of various organic molecules (AH₂) by H₂O₂ as its specific oxidant. It has been established^{1,2} that the reaction proceeds in a stepwise fashion via two intermediates called compounds **I** and **II**:



The first catalytic intermediate, compound **I**, has been extensively studied by resonance Raman (RR) spectroscopy.^{3–6} Nonetheless, considerable disagreement still exists in the

observed spectra of compound **I** (see ref 7 for a review) due to its instability at neutral pH and its high photosensitivity. Previous RR studies on the second catalytic intermediate, compound **II**, have revealed that compound **II** is active when the distal histidine (His-42 for HRP) is protonated and its N_ε-proton is hydrogen-bonded to the oxygen atom of the ferryl-oxo heme.^{8,9} The reactivity of compound **II** has been suggested to depend on the presence or absence of this hydrogen bond. The protonation/deprotonation of His42 has been investigated by RR spectroscopy in terms of the “heme-linked ionization” for the ferric,¹⁰ ferrous,¹¹ compound **I**,¹² compound **II**,^{8,9,13} and ferric CN-bound forms.^{14,15} The ¹H NMR studies by La Mar and co-

(3) Van Wart, H. E.; Zimmer, J. *J. Am. Chem. Soc.* **1985**, *107*, 3379–3381.

(4) Oertling, W. A.; Babcock, G. T. *J. Am. Chem. Soc.* **1985**, *107*, 6406–6407. (b) Oertling, W. A.; Babcock, G. T. *Biochemistry* **1985**, *27*, 3331–3338.

(5) Palaniappan, V.; Terner, J. *J. Biol. Chem.* **1989**, *264*, 16046–16055.

(6) Ogura, T.; Kitagawa, T. *Rev. Sci. Instrum.* **1988**, *59*, 1316–1320.

(7) Kitagawa, T.; Mizutani, Y. *Coord. Chem. Rev.* **1994**, *135*, 685–735.

(8) Hashimoto, S.; Tatsuno, Y.; Kitagawa, T. *Proc. Natl. Acad. Sci. U.S.A.* **1986**, *83*, 2417–2421.

(9) Sitter, A. J.; Reczek, C. M.; Terner, J. *J. Biol. Chem.* **1985**, *260*, 7515–7520.

(10) Smulevich, G.; Paoli, M.; Burke, J. F.; Sanders, S. A.; Thorneley, R. N. F.; Smith, A. T. *Biochemistry* **1994**, *33*, 7398–7407.

(11) Teraoka, J.; Kitagawa, T. *J. Biol. Chem.* **1981**, *256*, 3969–3977.

(12) Paeng, K.; Kincaid, J. R. *J. Am. Chem. Soc.* **1988**, *110*, 7913–7915.

[†] The abbreviations used are as follows: HRP, horseradish peroxidase; CcP, cytochrome *c* peroxidase; ARP, *Arthromyces ramosus* peroxidase.

[‡] Okazaki National Research Institutes.

[§] Kyoto University.

[⊥] Present address: Department of Biochemistry, School of Medicine, Keio University, Tokyo 160, Japan.

[⊗] Abstract published in *Advance ACS Abstracts*, February 1, 1997.

(1) Dunford, H. B. In *Peroxidases in Chemistry and Biology*; Everse, J. E., Everse K. E., Grisham, M. B., Eds.; CRC Press: Boca Raton, FL, 1991; Vol. II, pp 1–24.

(2) Yamazaki, I.; Tamura, M.; Nakajima, R. *Mol. Cell. Biochem.* **1981**, *40*, 143.

workers¹⁶ have demonstrated that the protonated imidazolium side chain of His42 serves as a hydrogen bond donor to the iron-bound cyanide. Recently, however, a report on the CO adduct of HRP reported that the pK_a of His42 is much lower (~ 4.0) and some unknown residue in the hydrogen bond network is responsible for the heme-linked ionization.¹⁷

X-ray crystallographic structures of various peroxidases including cytochrome *c* peroxidase (CcP)¹⁸ and *Arthromyces ramosus* peroxidase (ARP)¹⁹ indicate the presence of a hydrogen bond at the N_δ -side of the distal histidine. Although there is no crystallographic data for HRP, the sequence analysis²⁰ implicated that Asn70 of HRP serves as a hydrogen bond acceptor of the N_δ -proton of His42 which is a general acid–base catalyst in the reaction with hydrogen peroxide.¹⁸ Therefore, the hydrogen bond in the Asn70 \cdots His42 couple may function in a concerted way, playing an essential role in the enzymatic reaction despite the fact that Asn70 is located far from the heme. To investigate such hydrogen bond effects of the Asn70 \cdots His42 couple on the enzymatic activities, site-directed mutagenesis on Asn70 was carried out. It was found that Asn70 \rightarrow Val (N70V) and Asn70 \rightarrow Asp (N70D) mutants, in which the hydrogen bond of N_δ -proton is disrupted, have greatly reduced ($<10\%$ of native HRP) peroxidase activity.²¹ In addition, the pH dependence of the stability of compounds **I** and **II** of N70V HRP is quite different from that of native HRP; compound **I** is more stable than compound **II** at neutral pH, similar to ARP.²² In this study, we have explored the hydrogen-bonding effects of the Asn70 \cdots His42 couple on the active site structure of HRP by comparing the RR spectra of N70V and N70D HRP with that of native HRP each in the ferrous, ferric, ligand-bound ferric, and reaction intermediate forms.

Experimental Section

Materials. Native HRP (isozyme C) was purchased from Sigma (type VI) and used without further purification. The RZ value (A_{402}/A_{280} ratio) of this preparation was 3.2. The preparations of wild type (WT) and the mutant HRP were described in detail elsewhere.²¹ In brief, the proteins were expressed in *Escherichia coli*, extracted from inclusion bodies, reconstituted in the presence of Ca^{2+} and hemin to yield an active enzyme, and purified with ion-exchange chromatography.

The cyanide-bound form was obtained by addition of 18 mM $K^{12}C^{14}N$ (Wako Ltd.), $K^{12}C^{15}N$ (Cambridge Isotope Laboratories), or $K^{13}C^{14}N$ (Sigma-Aldrich, Japan) buffered solution to the 60 μM resting HRP in 50 mM sodium phosphate buffer at pH 7.0 to make the final concentration of KCN 600 μM . The pH value remained unchanged upon the addition of the cyanide solution. The formation of cyanoferric

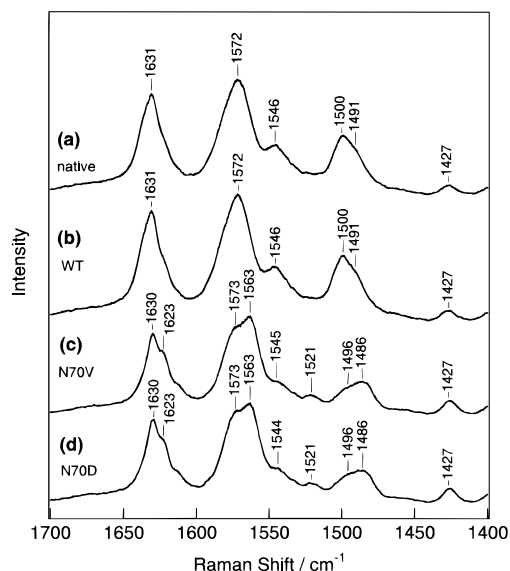


Figure 1. Resonance Raman spectra in the 1700–1400 cm^{-1} region of resting HRPs at pH 7.0: (a) native, (b) WT, (c) N70V, and (d) N70D. Excitation, 406.7 nm; laser power, ~ 15 mW; accumulation time, 2 min; enzyme concentration, 50 μM .

was confirmed with the UV–vis absorption spectrum before the RR measurements. Benzhydroxamic acid (BHA) adducts of HRPs were prepared by adding BHA to the ferric HRP solution so that the final BHA concentration could be 6 mM. The ferrous forms were obtained by addition of 3.0 μL of saturated sodium dithionite solution to 0.5 mL of the resting enzyme, and the reduction was confirmed by its UV–vis absorption spectrum. Buffer systems used for the measurements of pH dependent Fe^{II} –His stretching frequency were succinic acid–NaOH (pH 4–5), Na_2HPO_4 – NaH_2PO_4 (pH 5.7–8), and borate (pH 9–10). The pH values were determined for the solution in a Raman cell with a Beckman pH meter (model $\Phi 34$).

Compound **II** was prepared by mixing a slight excess amount of hydrogen peroxide with the resting HRP solution in the presence of 0.1 equiv of ferrocyanide in the case of native and wild type HRPs, but without ferrocyanide for the mutants. The integrity of compound **II** was confirmed by UV–vis absorption spectra before and after the measurements of RR spectra. $H_2^{18}O_2$ was prepared from $^{18}O_2$ as described by Sawaki and Foote.²³ The ^{18}O -content of the hydrogen peroxide was determined to be 92% by epoxidation of menadione.²⁴ The UV–vis absorption spectra were observed with a Hitachi 220S spectrophotometer.

Resonance Raman Spectroscopy. Raman scattering was excited at 406.7 and 413.1 nm by a Kr^+ ion laser (Spectra Physics Model 2016) and at 441.6 nm by a He/Cd laser (Kinmon Electronics Model CD1805B), and detected by an intensified photodiode array (PAR 1421HQ) attached to a single polychromator (Ritsu Oyo Kogaku, DG-1000) or a charge-coupled device (CCD) (PAR 1530-CUV) attached to a single polychromator (Chromex 250IS). The slit width was 100–200 μm . RR spectra were measured with a quartz spinning cell at room temperature except for compound **II**, which was measured at ~ 10 $^\circ C$ by flushing with cooled N_2 gas against the spinning cell. Raman shifts were calibrated to an accuracy of 1 cm^{-1} with CCl_4 and indene as frequency standards.

EPR Spectroscopy. Electron paramagnetic resonance (EPR) spectra were measured at 5 K with the X-band microwave frequency (9.35 GHz). The concentration of the samples was 200 μM .

Results

Figure 1 shows the RR spectra of native (a), wild-type (b), N70V (c), and N70D (d) HRPs at pH 7.0 excited at 406.7 nm. The ν_2 , ν_3 , and ν_{10} bands, which are observed at 1572, 1500, and 1631 cm^{-1} , respectively, for native HRP, are broader for

(23) Sawaki, Y.; Foote, C. S. *J. Am. Chem. Soc.* **1979**, *101*, 6292–6296.

(24) Ortiz de Montellano, P. R.; Catalano, C. E. *J. Biol. Chem.* **1985**, *260*, 9265–9271.

(13) Makino, R.; Uno, T.; Nishimura, Y.; Iizuka, T.; Tsuboi, M.; Ishimura, Y. *J. Biol. Chem.* **1986**, *261*, 8376–8382.

(14) Lopez-Garriga, J. J.; Oertling, W. A.; Kean, R. T.; Hoogland, H.; Wever, R.; Babcock, G. T. *Biochemistry* **1990**, *29*, 9387–9395.

(15) Al-Mustafa, J.; Kincaid, J. R. *Biochemistry* **1994**, *33*, 2191–2197.

(16) Thanabal, V.; de Ropp, S. J.; La Mar, G. N. *J. Am. Chem. Soc.* **1988**, *110*, 3027–3035.

(17) Holzbaier, I. E.; English, A. M.; Ismail, A. A. *J. Am. Chem. Soc.* **1996**, *118*, 3354–3359.

(18) Poulos, T. L.; Kraut, J. *J. Biol. Chem.* **1980**, *255*, 8199.

(19) (a) Kunishima, N.; Fukuyama, K.; Matsubara, H.; Hatanaka, H.; Shibano, Y.; Amachi, T. *J. Mol. Biol.* **1994**, *235*, 331–334. (b) Kunishima, N.; Amada, F.; Fukuyama, K.; Kawamoto, M.; Matsunaga, T.; Matsubara, H. *FEBS Lett.* **1996**, *378*, 291–294. (c) Fukuyama, K.; Kunishima, N.; Amada, F.; Kubota, T.; Matsubara, H. *J. Biol. Chem.* **1995**, *270*, 21884–21892.

(20) Welinder, K. G. *Eur. J. Biochem.* **1985**, *151*, 497–504.

(21) (a) Nagano, S.; Tanaka, M.; Watanabe, Y.; Morishima, I. *Biochem. Biophys. Res. Commun.* **1995**, *207*, 417–423. (b) Nagano, S.; Tanaka, M.; Ishimori, K.; Watanabe, Y.; Morishima, I. *Biochemistry* **1996**, *35*, 14251–14258. (c) Tanaka, M.; Nagano, S.; Ishimori, K.; Watanabe, Y.; Morishima, I. To be submitted.

(22) Farhangrazi, Z. S.; Copeland, B. R.; Nakayama, T.; Amachi, T.; Yamazaki, I.; Powers, L. S. *Biochemistry* **1994**, *33*, 5647–5652.

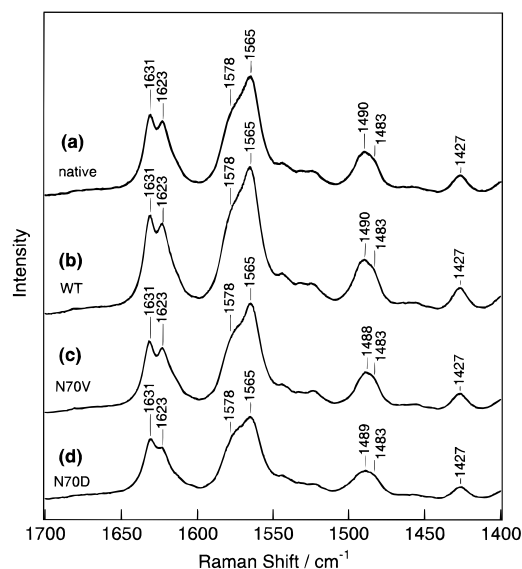


Figure 2. Resonance Raman spectra in the 1700–1400 cm^{-1} region of the BHA-adducts of ferric HRP at pH 7.0: (a) native, (b) WT, (c) N70V, and (d) N70D. Excitation, 406.7 nm; laser power, ~ 15 mW; accumulation time, 2 min; enzyme and BHA concentrations, 50 μM and 1 mM, respectively.

N70V and N70D mutants and seem to have other components at 1563, 1486, and 1623 cm^{-1} . The RR spectrum of native HRP is in agreement with those reported previously,^{11,25–27} and the ν_2 , ν_3 , and ν_{10} frequencies are indicative of a five-coordinate high-spin (5c-HS) heme. No detectable RR spectral difference was noticed between native and WT HRPs. The RR spectra of N70V and N70D HRPs are alike and close to that of F41V HRP reported by Smulevich *et al.*¹⁰ The frequencies of additional bands of N70V and N70D HRPs are suggestive of the presence of a six-coordinate high-spin (6c-HS) heme.

To confirm the appearance of the 6c-HS heme, the RR spectra of the BHA adducts were examined, and the results are displayed in Figure 2. The main components of the ν_2 and ν_3 bands of native HRP are shifted to 1565 and 1490 cm^{-1} , respectively, and a new band appeared at 1623 cm^{-1} , in agreement with the reported RR spectra.^{10,11,27,28} These RR spectral changes have been attributed to the formation of the 6c-HS heme.¹¹ Accordingly, it is reasonable to assign the additional bands of N70V and N70D HRPs in Figure 1 to the 6c-HS heme, presumably with a water molecule at the sixth coordination position. Since the BHA-free resting N70V and N70D HRPs are mixtures of the 5c-HS and 6c-HS species, the RR spectral pattern is scarcely altered by addition of BHA, although the frequencies of the 6c-HS marker bands are slightly different between spectra in Figures 1 and 2 owing to different axial ligands. The observed frequencies of these marker bands of the resting and BHA-bound HRPs are summarized in Table 1.

The EPR spectra of the native and the mutant HRPs were measured to explore differences in the ligand field symmetry around the iron. Figure 3 depicts the EPR spectra observed at 5 K for the resting state. The native (a) and WT (b) species gave essentially identical spectra with prominent rhombic high-spin splitting ($g = 6.45$ and 5.32). N70V (c) and N70D HRPs (d) also exhibited the rhombic high-spin splitting, but the

Table 1. Comparison of Key RR Frequencies for the Ferric Form of HRPs

species	ferric		ferric BHA complex	
	ν_2	ν_3	ν_2	ν_3
native	1572	1500, ^a 1491	1565, 1578	1491, 1483
wild type	1572	1500, 1491	1566, 1579	1491, 1484
N70V	1563, 1573	1486, 1496	1565, 1578	1490, 1483
N70D	1563, 1573	1486, 1496	1565, 1578	1491, 1483

^a The stronger lines are italic.

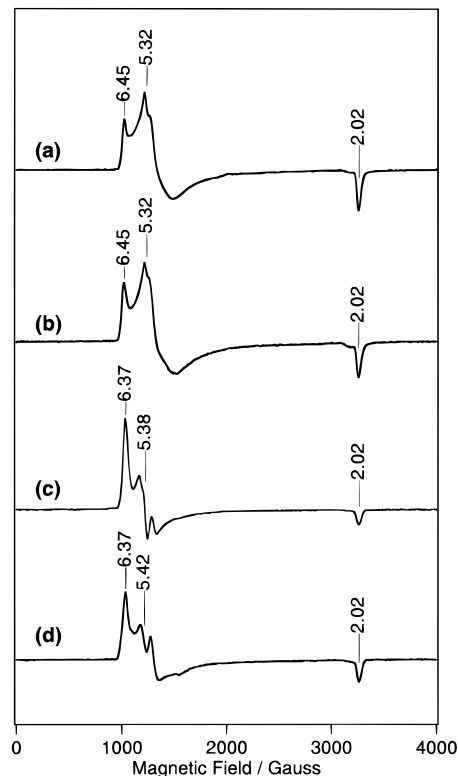


Figure 3. Electron paramagnetic resonance spectra of resting HRPs at 5 K: (a) native, (b) WT, (c) N70V, and (d) N70D. Enzyme concentration, 200 μM .

magnitude of splitting is appreciably reduced ($g = 6.37$ and 5.38–5.42). In the UV–vis absorption spectra, the extinction coefficient of the Soret band is increased to 120 and 125 $\text{mM}^{-1} \text{cm}^{-1}$ for N70V and N70D HRPs,²¹ respectively, compared with 102 $\text{mM}^{-1} \text{cm}^{-1}$ of native HRP. These observations are consistent with the coexistence of the 5c- and 6c-HS species in the mutants.

Figure 4 shows the RR spectra in the low-frequency region of reduced HRPs at pH 7.0 excited at 441.6 nm. The RR spectrum of the native species (a) is in agreement with that reported¹¹ and is characterized by an intense band at 242 cm^{-1} , which has been assigned to the Fe–histidine (proximal) stretching ($\nu_{\text{Fe-His}}$) vibration.¹¹ The $\nu_{\text{Fe-His}}$ band is usually observed around 220 cm^{-1} for histidine-coordinated reduced heme proteins but around 240 cm^{-1} for reduced peroxidases and appears only for the 5c-HS state upon excitation around 441 nm.²⁹ The $\nu_{\text{Fe-His}}$ bands of reduced N70V (c) and N70D (d) mutants appeared at lower frequencies by 4 cm^{-1} than that of native HRP, while all other bands did not exhibit a detectable frequency shift.

Since the $\nu_{\text{Fe-His}}$ mode of reduced HRP has been known to exhibit pH dependent frequency shifts,¹¹ RR spectra were

(25) Rakhit, G.; Spiro, T. G. *Biochemistry* **1974**, *13*, 5317–5323.

(26) Sievers, G.; Osterlund, K.; Ellfolk, N. *Biochim. Biophys. Acta* **1979**, *581*, 1–14.

(27) Smulevich, G.; English, A. M.; Mantini, A. R.; Marzocchi, M. P. *Biochemistry* **1991**, *30*, 772–779.

(28) Kitagawa, T.; Hashimoto, S.; Teraoka, J.; Nakamura, S.; Yajima, H.; Toichiro, H. *Biochemistry* **1983**, *22*, 2788.

(29) Kitagawa, T. In *Biological Applications of Raman Spectroscopy*; Spiro, T. G., Ed.; John Wiley & Sons: New York, 1988; Vol. 3, pp 97–131.

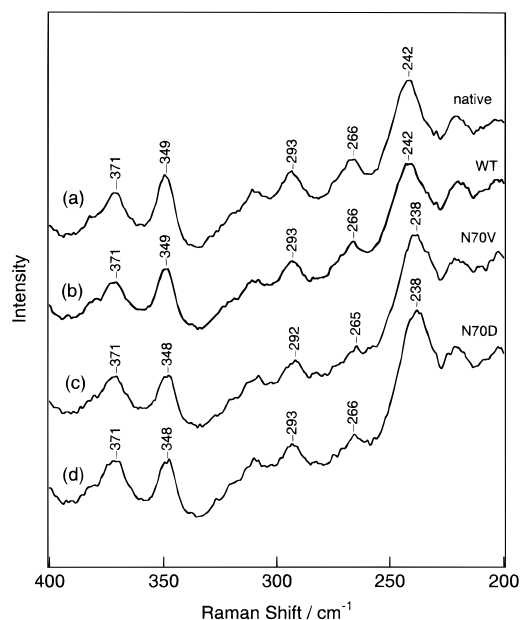


Figure 4. Resonance Raman spectra in the 400–200 cm^{-1} region of reduced HRPs at pH 7.0: (a) native, (b) WT, (c) N70V, and (d) N70D. Excitation, 441.6 nm; laser power, ~ 14 mW; accumulation time, 3 min; enzyme concentration, 60 μM .

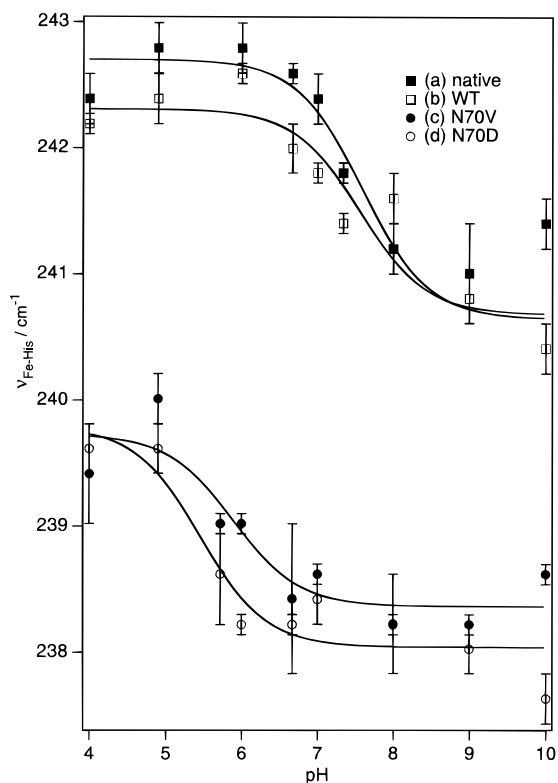


Figure 5. pH dependence of the $\nu_{\text{Fe-His}}$ frequencies of reduced HRPs: (a) native, (b) WT, (c) N70V, and (d) N70D. The solid lines denote theoretical titration curves for a single proton, which were fitted to the experimental points by a nonlinear least-squares method.

measured at different pHs for reduced HRPs. If the two $\nu_{\text{Fe-His}}$ bands at different frequencies, corresponding to protonated and deprotonated forms, have the same intrinsic intensities and are not resolved, the apparent peak position reflects the relative population of the two species. Accordingly, the observed $\nu_{\text{Fe-His}}$ frequencies are plotted against pH in Figure 5, where solid lines stand for the single-proton titration curves fitted to the experimental points, which were calculated with a nonlinear least-

squares procedure. The $\nu_{\text{Fe-His}}$ bands of native and WT HRPs shift to lower frequencies at higher pH with the midpoint pH of 7.2. Similar fitting of the $\nu_{\text{Fe-His}}$ frequencies yielded the midpoint pH values of 5.9 for N70V and 5.5 for N70D HRPs. Thus, it became evident that both the native and the mutant HRPs exhibit the pH dependent frequency shifts of the $\nu_{\text{Fe-His}}$ mode and the amounts of frequency shifts are similar but their midpoint pH values are distinct.

Figure 6 shows the RR spectra in the 550–250 cm^{-1} region of $^{12}\text{C}^{14}\text{N}$ (A), $^{12}\text{C}^{15}\text{N}$ (B), and $^{13}\text{C}^{14}\text{N}$ (C) adducts of native (a), WT (b), N70V (c) and N70D (d) oxidized HRPs at pH 7.0 excited at 413.1 nm. The broken lines denote the spectra between 470 and 320 cm^{-1} calculated under the assumption that bands with a Gaussian band shape are present at the frequencies of marked values. The relative peak heights and widths of individual bands for the three isotope species of native HRP are listed in Table 2. Only when the assumed frequencies differ from the values shown for the top spectra, the assumed values are designated for individual bands of spectra b–d. Since the broken lines are almost overlapped with the solid lines, their differences are not clear in Figure 6. The broad bands of native and WT HRP- $^{12}\text{C}^{14}\text{N}$ at 450 cm^{-1} (Figure 6A, a,b) are shifted to 446–447 cm^{-1} for the $^{12}\text{C}^{15}\text{N}$ (Figure 6B, a,b) and $^{13}\text{C}^{14}\text{N}$ adducts (Figure 6C, a,b). The bands of the native and WT HRP- $^{12}\text{C}^{14}\text{N}$ at 417 and 402 cm^{-1} are shifted to 413 and 400 cm^{-1} , respectively, for $^{13}\text{C}^{14}\text{N}$ adducts but are not shifted with $^{12}\text{C}^{15}\text{N}$ adducts.

These frequency shifts are more clearly seen in the isotope-difference spectra shown in Figure 7, where the differences $^{12}\text{C}^{14}\text{N} - ^{12}\text{C}^{15}\text{N}$ (A) and $^{12}\text{C}^{14}\text{N} - ^{13}\text{C}^{14}\text{N}$ (B) are depicted. The solid lines and broken lines in Figure 7 represent the differences among solid lines and broken lines in Figure 6, respectively. The 455/443 cm^{-1} pair for $^{12}\text{C}^{14}\text{N}/^{12}\text{C}^{15}\text{N}$ is assigned to the Fe–CN stretching ($\nu_{\text{Fe-CN}}$) mode of oxidized HRP, and the corresponding bands are observed at 450/435 cm^{-1} for N70V (Figure 7 A, c) and at 450/434 cm^{-1} for N70D (Figure 7A, d), although they are too weak to be identified in the raw spectra (Figure 6A,B). Thus, the $\nu_{\text{Fe-CN}}$ bands appear at appreciably lower frequencies for the mutants than that for the native species. The other isotope-sensitive bands at 418/411 and 403/397 cm^{-1} for $^{12}\text{C}^{14}\text{N}/^{13}\text{C}^{14}\text{N}$ (Figure 7B) are insensitive to the N isotope, in agreement with the reported results,^{14,15} and therefore are assignable to δ_{FeCN} . Note that the frequencies of δ_{FeCN} modes are little shifted by Asn70 mutation. The difference peaks around 390–360 cm^{-1} in Figure 7 will be discussed later.

Figure 8 shows the RR spectra of compound **II** derived from $\text{H}_2^{16}\text{O}_2$ (A) and $\text{H}_2^{18}\text{O}_2$ (B) generated in D_2^{16}O at pD 7.0, which were excited at 406.7 nm. A Raman band of native HRP at 775 cm^{-1} (A, a) has been assigned to the $\text{Fe}^{\text{IV}}=\text{O}$ stretching ($\nu_{\text{Fe=O}}$) mode. The corresponding bands for N70V and N70D HRPs are observed at 779 cm^{-1} for the $\text{H}_2^{16}\text{O}_2$ derivative and 748 cm^{-1} for the $\text{H}_2^{18}\text{O}_2$ derivative. Although the intensity of the 779 cm^{-1} band for N70V HRP is considerably weaker than that for native HRP, its presence is demonstrated in the oxygen isotope-difference spectra shown in Figure 8C. It is apparent that the $\nu_{\text{Fe=O}}$ frequencies of compound **II** of N70V and N70D mutants at pD 7.0 are upshifted by 5–6 cm^{-1} compared to those of native and WT HRPs. It is also noted that the 774 cm^{-1} band in Figure 8B, a, arises from the $\text{Fe}=\text{O}$ species, which is generated by the oxygen atom exchange with bulk water after the formation of the $\text{Fe}=\text{O}$ heme,⁸ and this kind of oxygen exchange is also seen for the N70D mutant at pD 7.0.

Similar experiments were carried out at pD 10.0, and the results are shown in Figure 9. The $\nu_{\text{Fe=O}}$ band, observed at

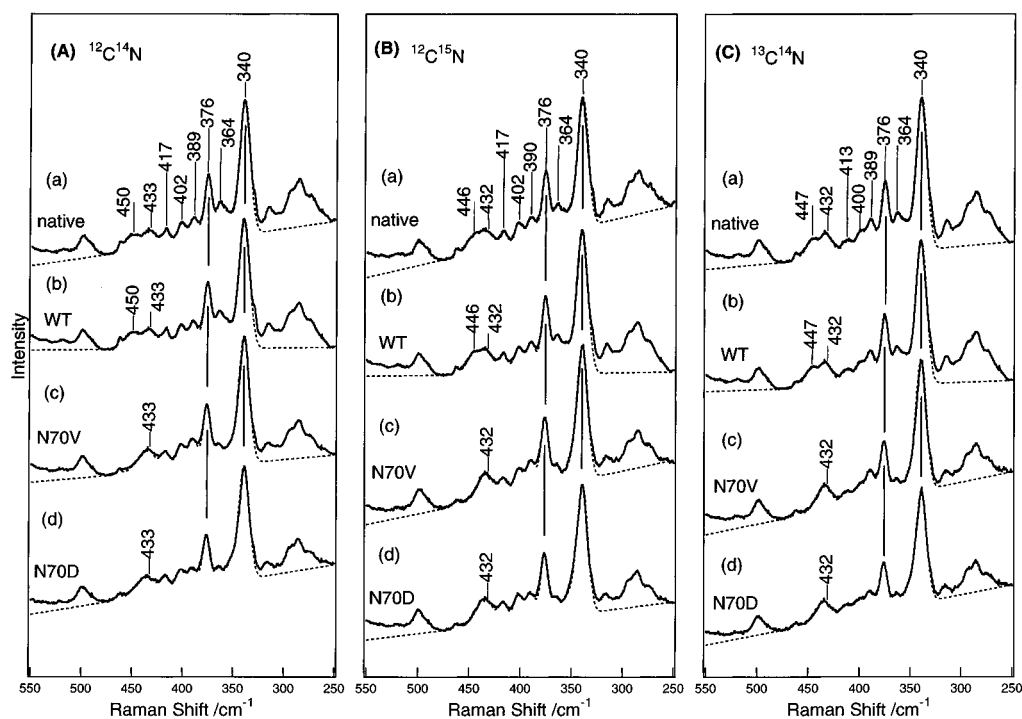


Figure 6. Resonance Raman spectra in the 550–250 cm^{-1} region of CN-adducts of resting HRPs at pH 7.0: (A) $^{12}\text{C}^{14}\text{N}$ adducts, (B) $^{12}\text{C}^{15}\text{N}$ adducts, (C) $^{13}\text{C}^{14}\text{N}$ adducts; (a) native, (b) WT, (c) N70V, and (d) N70D. Excitation, 413.1 nm; laser power, 22 mW; accumulation time, 10 min; enzyme concentration, 60 μM . Broken lines denote the simulated spectra under the assumption that bands with a Gaussian band shape are present at the designated frequencies. The peak heights and band widths of the assumed bands are listed in Table 2. Only when the assumed frequencies are different from those shown for the top spectra, the assumed frequency is designated at each peak.

Table 2. Simulation Constants of RR Spectra for HRP-CN with Gaussian Band Shapes

	$^{12}\text{C}^{14}\text{N}$			$^{13}\text{C}^{14}\text{N}$			$^{12}\text{C}^{15}\text{N}$		
	frequency ^a	intensity ^b	$\Delta_{1/2}$ ^c	frequency ^a	intensity ^b	$\Delta_{1/2}$ ^c	frequency ^a	intensity ^b	$\Delta_{1/2}$ ^c
native	340	100	6.2	340	100	6.2	340	100	6.2
	355	14	6.7	355	16	6.7	353	13	6.0
	364	23	5.0	364	20	5.0	364	20	5.0
	376	48	4.5	376	47	4.5	376	50	4.5
	389	18	5.0	389	22	5.4	390	18	5.4
	402	15	5.2	400	15	5.2	402	15	5.4
	417	11	5.8	413	11	6.7	417	11	4.6
	433	12	6.5	432	15	6.8	432	11	6.8
	450	14	9.2	447	15	8.3	446	17	8.5

^a In cm^{-1} . ^b Relative height at band center. ^c Half-height at half-width in cm^{-1} .

775 cm^{-1} for native and WT HRPs at pD 7.0 in Figure 8A, a,b, is upshifted to 785 cm^{-1} at pD 10.0, as displayed by traces (a) and (b) in Figure 9A. This band exhibits a downshift by 30 cm^{-1} upon ^{18}O isotope substitution as shown by traces (a) and (b) in Figure 9B. The $\nu_{\text{Fe}=\text{O}}$ bands of compound **II** of N70V and N70D HRPs at pD 10.0 are observed at 781 cm^{-1} for the $\text{H}_2^{16}\text{O}_2$ derivative (Figure 9A) and are shifted to 748 cm^{-1} for the $\text{H}_2^{18}\text{O}_2$ derivative (Figure 9B). This means that the $\nu_{\text{Fe}=\text{O}}$ band of native HRP compound **II** exhibits an upshift of 10 cm^{-1} upon raising the pH from 7 to 10, but those of N70V and N70D mutants show very small pH dependent frequency shifts. In Figure 8B, a, the 774 cm^{-1} band, corresponding to the $\text{Fe}=\text{O}$ heme, was observed for the $\text{H}_2^{18}\text{O}_2$ derivative, but such a feature is not seen in Figure 9B, a, indicating that the oxygen exchange does not occur at pD 10.0. The same is true for the N70D mutant.

Since the frequency shift of the native HRP has been explained by deletion of the hydrogen bond between the oxygen atom of the ferryl-oxo heme and His42 owing to its deprotonation,^{8,9,13} the very small frequency shift of $\nu_{\text{Fe}=\text{O}}$ of the mutant HRPs may suggest either the presence of the hydrogen bond (even at pD 10.0) or its absence at pD 7.0. In order to clarify

whether the hydrogen bond between His42 and the oxygen atom of the ferryl-oxo heme is present or not, we tried to observe the H/D effects on the $\nu_{\text{Fe}=\text{O}}$ frequency, which should exhibit a small frequency shift in the presence of this hydrogen bond. Due to unknown reasons, the $\nu_{\text{Fe}=\text{O}}$ bands of compound **II** of HRPs in H_2O solutions are too broad to be identified in the raw spectra (3 times broader in H_2O than in D_2O). Therefore, we calculated the $^{16}\text{O}/^{18}\text{O}$ -difference spectra and compared them. For this purpose the grating of the spectrometer was replaced with one providing higher resolution (900 nm blaze, 1200 grooves/mm, being used in the second order). The oxygen isotope-difference spectra observed for the H_2O and D_2O solutions under the same conditions are presented in Figure 10, where spectra (a), (c), (e), and (g) show the $^{16}\text{O}/^{18}\text{O}$ difference spectra of native, WT, N70V, and N70D HRPs in D_2O , respectively, and spectra (b), (d), (f), and (h) denote the corresponding spectra for H_2O solutions. It is apparent that D_2O solutions give rise to stronger RR bands than H_2O solutions. The frequencies of positive and negative peaks for spectrum (a) agree with those of spectrum (b), and the frequencies of spectrum (c) agree with those of spectrum (d) within 1 cm^{-1} . This means that the $\nu_{\text{Fe}=\text{O}}$ frequencies in the H_2O and D_2O solutions are identical for native

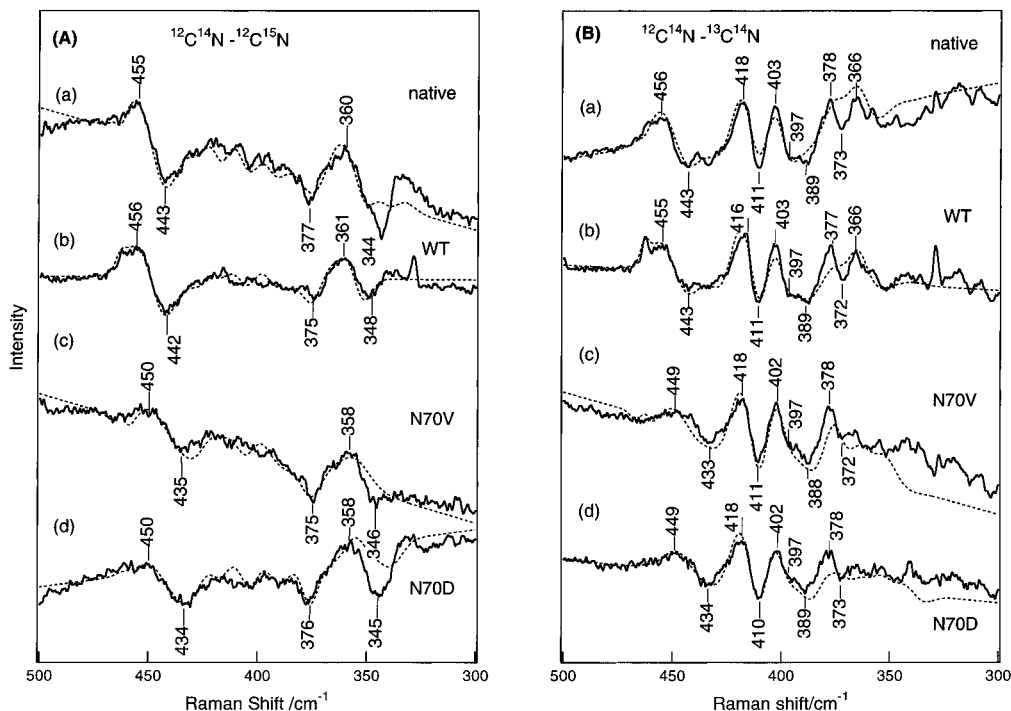


Figure 7. Isotope-difference spectra for the spectra shown in Figure 6: (A) $^{12}\text{C}^{14}\text{N} - ^{12}\text{C}^{15}\text{N}$ and (B) $^{12}\text{C}^{14}\text{N} - ^{13}\text{C}^{14}\text{N}$. The solid lines and broken lines denote the differences corresponding to the solid lines and broken lines of Figure 6, respectively.

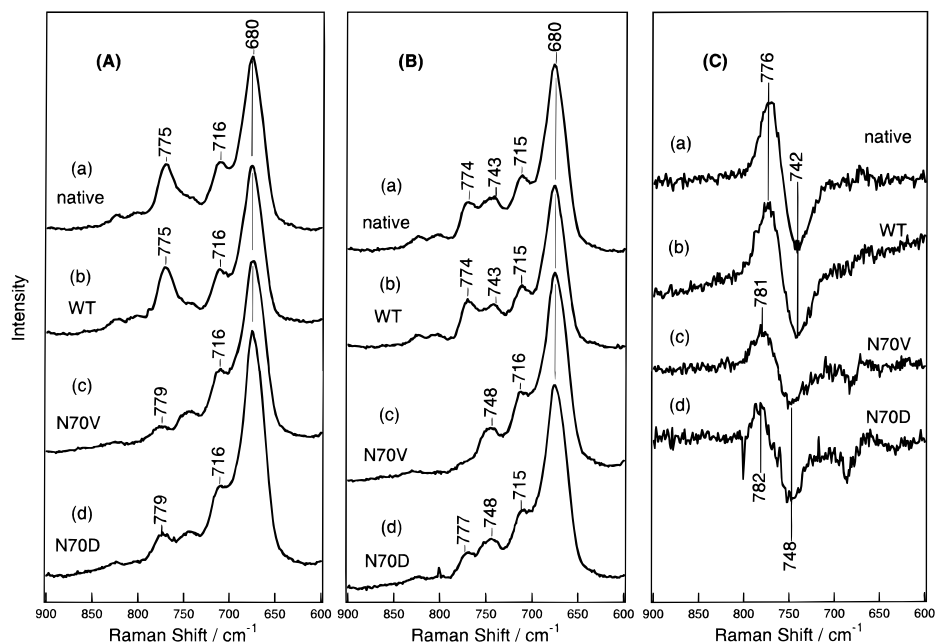


Figure 8. Resonance Raman spectra in the 900–600 cm^{-1} region of compound **II** in D_2^{16}O at pD 7.0 and their differences: (A) derived from $\text{H}_2^{16}\text{O}_2$, (B) derived from $\text{H}_2^{18}\text{O}_2$, (C) $\text{H}_2^{16}\text{O}_2 - \text{H}_2^{18}\text{O}_2$; (a) native, (b) WT, (c) N70V, and (d) N70D. Excitation, 406.7 nm; laser power, ~ 14 mW; accumulation time, 1 min; enzyme concentration, 60 μM .

and WT HRPs. In contrast, the negative peak positions of N70V and N70D HRPs are higher in D_2O than in H_2O by 4 cm^{-1} while positive peak positions are higher by 1 cm^{-1} . The $\nu_{\text{Fe}=\text{O}}$ frequencies and the deuteration shifts observed are summarized in Table 3.

Discussion

Acid–Base Transition of His42 in the Reduced State. The X-ray crystallographic structure in the neighborhood of the heme of CcP¹⁸ is reproduced in Figure 11, where the residue numbers in parentheses stand for those of HRP.²⁰ There is a hydrogen bond network for His42 \cdots Asn70 \cdots Gln64 in the distal side of

HRP and a strong hydrogen bond between $\text{N}_\delta\text{-H}$ of His170 and the carboxylic side chain of Asp247 in the proximal side. There is no direct interaction between His42 and the heme iron of reduced HRP. Nevertheless, the Fe–His(proximal) stretching RR band of reduced native HRP exhibits pH dependent frequency shifts with the midpoint pH of 7.2 (Figure 5), which closely agrees with the pK_a of His42 of reduced HRP isozyme C determined from the proton balance experiment ($\text{pK}_a = 7.17$)³⁰ and from the redox potential measurement ($\text{pK}_a = 7.32$).³¹ Therefore, it has been inferred that the pH dependent frequency

(30) Yamada, H.; Yamazaki, I. *Arch. Biochem. Biophys.* **1974**, *165*, 728–738.

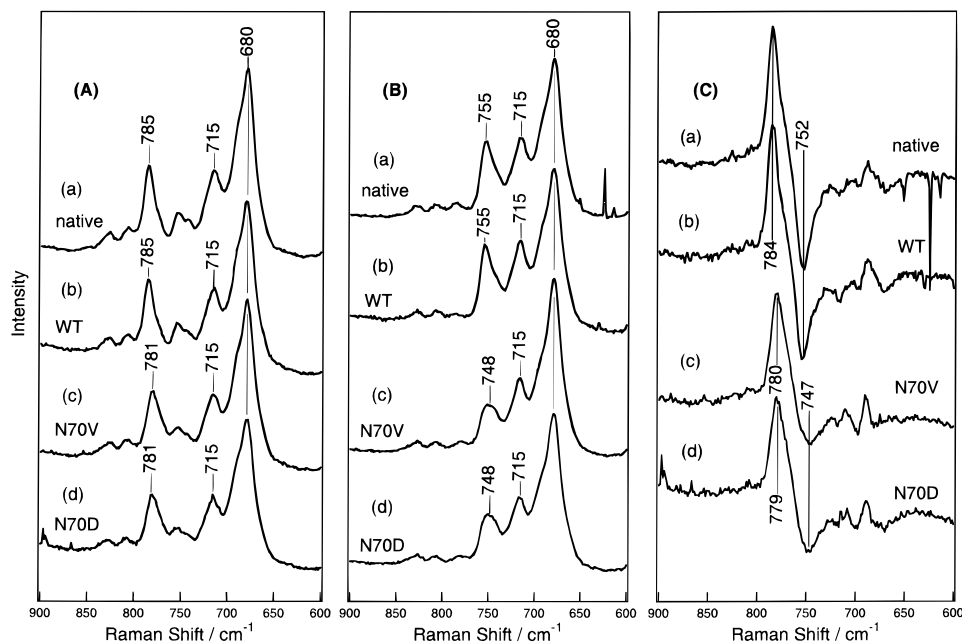


Figure 9. Resonance Raman spectra in the 900–600 cm^{-1} region of compound **II** in D_2^{16}O at pH 10.0 and their differences: (A) derived from $\text{H}_2^{16}\text{O}_2$, (B) derived from $\text{H}_2^{18}\text{O}_2$, (C) $\text{H}_2^{16}\text{O}_2 - \text{H}_2^{18}\text{O}_2$; (a) native, (b) WT, (c) N70V, and (d) N70D. Excitation, 406.7 nm; laser power, ~ 14 mW; accumulation time, 3 min; enzyme concentration, 60 μM .

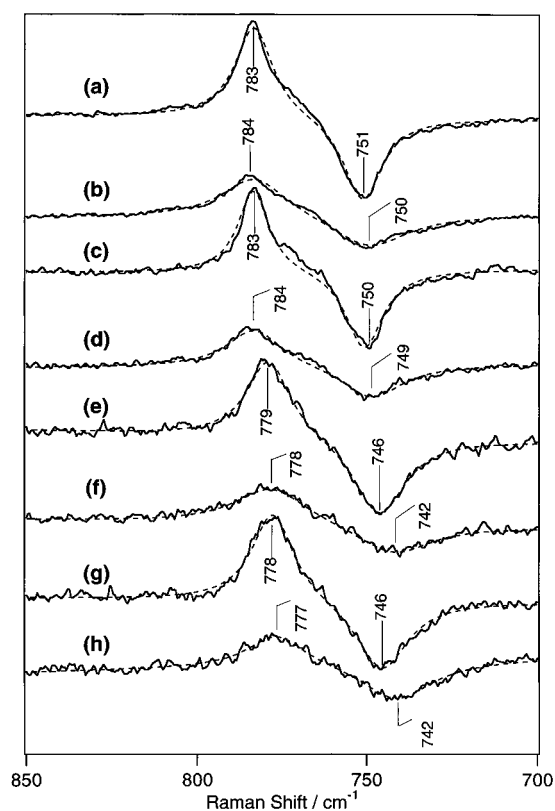


Figure 10. ^{16}O minus ^{18}O difference spectra of compound **II** in H_2^{16}O and D_2^{16}O at pH(D) 10.0: (a) native in H_2O , (b) native in D_2O , (c) WT in H_2O , (d) WT in D_2O , (e) N70V in H_2O , (f) N70V in D_2O , (g) N70D in H_2O , and (h) N70D in D_2O . Excitation, 406.7 nm; laser power, ~ 14 mW; accumulation time, 3 min; enzyme concentration, 60 μM .

change of the $\nu_{\text{Fe}-\text{His}}$ band originates from a deprotonation of the distal His.¹¹ The deprotonation would cause a small conformational change of the distal His, which is not localized in the distal side of ferrous HRP.

Table 3. Deuteration Shifts of the $\text{Fe}^{\text{IV}}=\text{O}$ Stretching Mode

enzyme	$\nu_{\text{Fe}=\text{O}}^{16\text{O}}/\text{cm}^{-1}$			$\nu_{\text{Fe}=\text{O}}^{18\text{O}}/\text{cm}^{-1}$		
	in D_2O	in H_2O	$\Delta\nu$	in D_2O	in H_2O	$\Delta\nu$
native	783	784	-1	751	750	1
wild type	783	784	-1	750	749	1
N70V	779	778	1	746	742	4
N70D	778	777	1	746	742	4

Holzbar et al.¹⁷ examined the pH dependence of IR $\text{C}=\text{O}$ stretching bands of the CO-adduct of ferrous HRP and ascribed a change at pH 8.7 to alteration in a hydrogen-bonding network triggered by deprotonation of Arg38. Since CO is in the distal side, the hydrogen bond network might be different from that communicating to the proximal side. On the other hand, Smulevich et al.¹⁰ have pointed out that the acid–base transition of the distal histidine of reduced CcP is communicated to the Fe–His bond in the proximal side through the hydrogen bond network of $\text{Trp51}\cdots\text{Arg48}\cdots\text{heme propionate}\cdots\text{His181}$. Through the analogous hydrogen bond network, the conformational change of the imidazole group of distal His of ferrous HRP would be communicated to the proximal His and/or heme propionate, resulting in a change of strain of the Fe–His bond (Scheme 1a). A similar conformational change of protein is induced by an acid–base transition of a histidine residue (His48) of RNase A.^{32,33}

The pH dependent frequency shift of $\nu_{\text{Fe}-\text{His}}$ also took place for reduced N70V and N70D mutants with a lower midpoint pH (5.5–5.9). Analogy to this consideration suggests that the pK_a of His42 is lowered to 5.5–5.9, owing to the lack of the hydrogen bond at the N_δ -position, as illustrated in Scheme 1b. Because of the absence of the hydrogen bond acceptor, the imidazolium cation is destabilized in the acidic form for the mutants and is deprotonated at a lower pH than for native HRP.

The hydrogen bond between His170 and the carboxylic side chain of Asp247 at the proximal side of HRP (Figure 11) is so strong that the Fe^{II} -coordinated imidazole becomes close to an imidazolate anion. Thus, the $\text{Fe}^{\text{II}}-\text{His}$ bond becomes stronger

(31) Yamada, H.; Makino, R.; Yamazaki, I. *Arch. Biochem. Biophys.* **1975**, *169*, 344–353.

(32) Cohen, J. S.; Shindo, H. *J. Biol. Chem.* **1975**, *250*, 8874–8881.

(33) Markley, J. L. *Biochemistry* **1975**, *14*, 3554–3561.

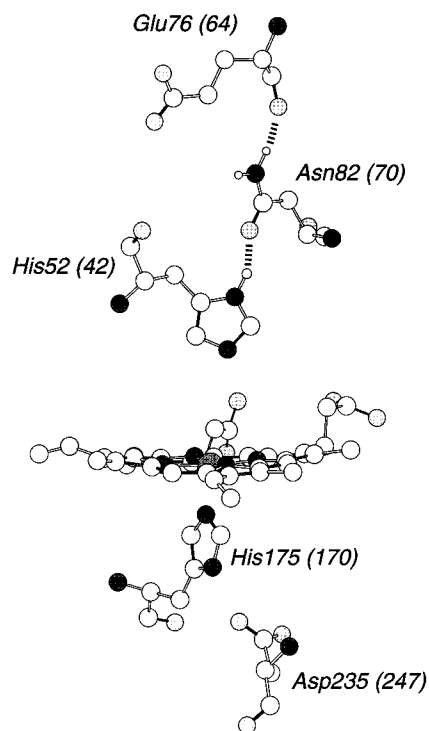
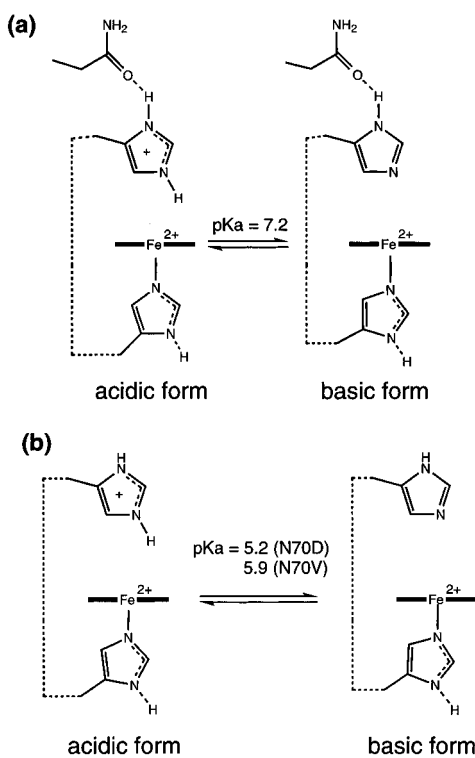


Figure 11. X-ray crystallographic structures of the heme proximity of CcP.¹⁸ The hydrogen bond is expressed by a hatched bond. Amino acid numbering is for CcP, but the numbers in parentheses denote the numbering for HRP.²⁰

Scheme 1. Acid–Base Transition in the Reduced HRP: (a) Native, (b) Mutants



and the $\nu_{\text{Fe-His}}$ frequency is raised.¹¹ This is the reason for the high $\nu_{\text{Fe-His}}$ frequency commonly seen for reduced peroxidases. The frequencies of $\nu_{\text{Fe-His}}$ for the mutants are lower than those of native HRP at the pH range we have examined. The deletion of the hydrogen bond between Asn70 and His42 may relax the protein structure and weaken the hydrogen bond between His170 and Asp247. The weakening of the hydrogen bond can

reasonably explain the lower frequency of $\nu_{\text{Fe-His}}$ in N70V and N70D mutants compared with that of native HRP.

Hydrogen Bond between His42 and Cyanide Ligand. In the cyanide-bound ferric heme of native HRP, His42 serves as a hydrogen bond donor to the cyanide ligand.^{16,19c,34,35} Al-Mustafa and Kincaid¹⁵ pointed out that the Fe–C–N moiety in the ferric HRP·CN yields two conformers, that is, linear and bent forms. The linear form gives a $\nu_{\text{Fe-CN}}$ band at 453 cm^{-1} at pH 5.5 and 444 cm^{-1} at pH 11.6, and this frequency shift of the linear form is ascribed to disruption of the hydrogen bond between His42 and the cyanide ligand, taking place at pH 10.6.¹⁵ The δ_{FeCN} mode of the linear form was assigned to the band at 405 cm^{-1} , and this band exhibited no frequency shift upon pH changes.¹⁵ The $\nu_{\text{Fe-CN}}$ and δ_{FeCN} modes of the bent form were assigned to the bands at 360 and 422 cm^{-1} , respectively, and these bands exhibited small frequency shifts ($\sim 2 \text{ cm}^{-1}$) upon pH changes.¹⁵

As demonstrated in Figures 6 and 7, the $\nu_{\text{Fe-CN}}$ and δ_{FeCN} bands have been observed with the present preparations. The 455/443 cm^{-1} pair in Figure 7A, a, corresponding to the $\nu_{\text{Fe-CN}}$ of the linear form, is shifted to lower frequencies by 5 cm^{-1} (to 450/435–434 cm^{-1}) for N70V and N70D (Figure 7A, c,d), although the amounts of the frequency shifts are difficult to determine precisely owing to weakness of the bands. We note that the weakening of bands and lower frequency shifts of the $\nu_{\text{Fe-CN}}$ band in N70V and N70D are in agreement with the changes of the $\nu_{\text{Fe-CN}}$ band of native HRP seen upon alkalization,¹⁵ in which N_c-H of His42 is deprotonated and the hydrogen bond between His42 and Fe^{III}-bound cyanide is disrupted. Accordingly, the $\nu_{\text{Fe-CN}}$ Raman characteristics of N70V and N70D HRPs seem to be interpreted in terms of deprotonation of His42. The ¹H NMR study of N70D HRP·CN, however, indicated that His42 is protonated similarly to native HRP·CN at pH 7.0.^{21c} Therefore, it is most likely that the imidazolium cation of His42 is not fixed at the position where it should be located in the presence of the hydrogen bond to Asn70, and as a result a hydrogen bond is not formed between His42 and the cyanide ligand of the ferric heme even though His42 is protonated.

The 418/411 and 403/397 cm^{-1} pairs for ¹²C¹⁴N/¹³C¹⁴N in Figure 7B, a, are in agreement with the frequencies of the δ_{FeCN} modes of the bent and linear forms, respectively.¹⁵ These frequencies are insensitive to Asn70 mutation. The difference peaks around 360 cm^{-1} in Figure 7A,B partly arise from the $\nu_{\text{Fe-CN}}$ mode of the bent form,¹⁵ but since this mode is coupled with porphyrin vibrations, the calculated spectra cannot reproduce the observed spectra and there appear complicated difference peak patterns. Similar features were recently reported for RR spectra of CN-adducts of Mb and Hb by Hirota et al.³⁶ Thus, most of the CN isotope-sensitive bands except for the $\nu_{\text{Fe-CN}}$ band of the linear form exhibited small frequency shifts upon mutation, and this is consistent with the observed features of pH dependences of the CN isotope-sensitive bands of native HRP·CN.¹⁵

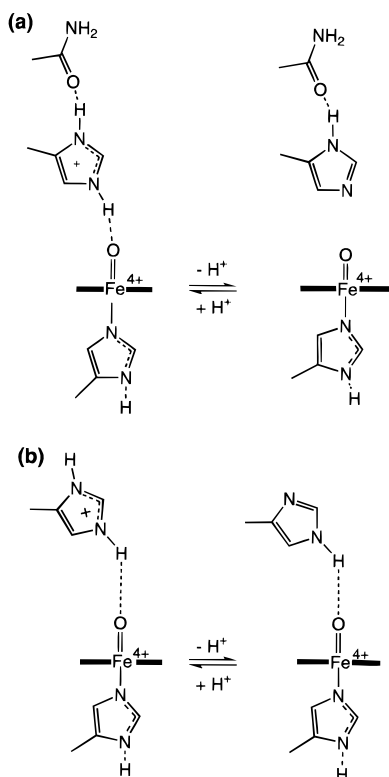
Hydrogen Bonding and Reactivity of Compound II. Previous RR^{8,9,13} and EXAFS³⁷ studies on compound II of native HRP demonstrated that the oxygen atom of the ferryl-oxo heme is hydrogen-bonded to His42 and the pH dependent frequency shift of $\nu_{\text{Fe=O}}$ shown in Figures 8 and 9 arises from deprotonation of His42. The reported pK_a of His42 for

(34) Edwards, S. L.; Poulos, T. L. *J. Biol. Chem.* **1990**, *265*, 2588–2595.

(35) Dunford, H. B. *Adv. Inorg. Biochem.* **1982**, *4*, 41–68.

(36) Hirota, S.; Ogura, T.; Shinzawa-Itoh, K.; Yoshikawa, S.; Kitagawa, T. *J. Phys. Chem.* **1996**, *100*, 15274–15279.

(37) Chang, C. S.; Yamazaki, I.; Sinclair, R.; Khalid, S.; Powers, L. *Biochemistry* **1993**, *32*, 923–928.

Scheme 2. Acid–Base Transition in Compound **II** of HRP: (a) Native, (b) Mutants.

compound **II** of HRP isozyme C is 8.8.⁸ The upshift of $\nu_{\text{Fe=O}}$ at alkaline pH is caused by rupture of the hydrogen bond. In contrast, the $\nu_{\text{Fe=O}}$ band of N70V and N70D mutants does not show similar pH dependent frequency shifts between pD 7.0 and pD 10.0. To determine whether the hydrogen bond persists until pD 10.0 or no hydrogen bond is formed at pD 7.0 for these mutants,³⁸ frequency differences of $\nu_{\text{Fe=O}}$ between the H₂O and D₂O solutions were examined with the higher resolution.

As displayed in Figure 10, the sizes of the D₂O/H₂O frequency shifts are similar to those reported for catalytic intermediates of native HRP at neutral pH (2 cm⁻¹ from ref 8 and 4 cm⁻¹ from refs 9 and 13). The presence of small but clear frequency shifts suggests that a weak hydrogen bond exists between N_ε-H of His42 and the oxygen atom of the ferryl oxo heme. The hydrogen bond becomes slightly weaker for the N_ε-D form than for the N_ε-H form, and as a result, the $\nu_{\text{Fe=O}}$ frequency becomes slightly higher in D₂O than in H₂O. The fact that the $\nu_{\text{Fe=O}}$ frequencies of N70V and N70D HRP are lower than those of native species is also consistent with the presence of the hydrogen bond.

The discussion mentioned above is illustrated in Scheme 2. In native HRP (Scheme 2a), deprotonation of His42 means removal of the N_ε-proton, retaining the N_δ-proton, and thus the hydrogen bond between His42 and the oxygen ligand is cleaved at alkaline pH. The cleavage of the hydrogen bond causes the shift of $\nu_{\text{Fe=O}}$ to a higher frequency from 775 cm⁻¹ at pD 7 to 785 cm⁻¹ at pD 10. The H₂O/D₂O frequency shift of $\nu_{\text{Fe=O}}$ is recognizable only at neutral pH for native HRP.^{8,9,13} In N70V and N70D HRP, on the other hand, the hydrogen bond between His42 and the oxygen ligand at pD 7.0 is significantly weaker

than that of native HRP at pD 7.0, as illustrated in Scheme 2b, presumably owing to the fact that His42 has slightly moved away from the normal position under the absence of the N_δ-hydrogen bond. Upon raising the pH, the N_δ-proton is deprotonated, keeping the N_ε-proton. Accordingly, the weak hydrogen bond between His42 and the oxygen ligand is retained at alkaline pH, and the H₂O/D₂O frequency shift of $\nu_{\text{Fe=O}}$ is observed even at pD 10.0.

The weak hydrogen bond between His42 and the oxygen ligand of compound **II** for N70V and N70D mutants would be expected to cause the oxygen exchange, since the hydrogen-bonded N_ε-proton combines with the oxygen ligand to yield a hydroxy anion in the oxygen exchange reaction with water. The oxygen exchange is confirmed by the presence of the Fe=O¹⁶O stretching RR band for the Fe=O¹⁸O sample at pD 7.0, but such an exchange reaction ceases to occur at pD 10.0. The stability of the ferryl oxo oxygen at pD 10.0 can be interpreted in the following way. Deprotonation of the N_ε-proton from the imidazolium cation of His42 forms neutral imidazole, but deprotonation of neutral His42 results in the formation of an imidazolyl anion. Therefore, the deprotonation of the N_δ-proton of His42 increases the effective pK_a value of the N_ε-proton, making instantaneous deprotonation from the N_ε atom more difficult. The higher effective pK_a of the N_ε-proton results in the formation of a less labile oxygen atom and thus makes the oxygen exchange less feasible.

Since the reduction of compound **II** is the rate-determining step of the peroxidase reaction cycle, the overall activity of the enzyme depends on the reactivity of compound **II**. The kinetic pK_a values for the reduction rate of compound **II** closely agree with the midpoint pH value of the acid–base transition of compound **II** arising from the presence or absence of the hydrogen bond between the N_ε-proton of His42 and the oxygen ligand. Moreover, the diacetylheme-substituted compound **II** of HRP, which has a weaker hydrogen bond between the distal His and ferryl oxygen owing to the cis-effects from the diacetyl groups, exhibited lower reactivity than native compound **II**.¹³ Consequently, the lower oxidation activity of these mutants against phenol derivatives in the steady state at neutral pH^{21a,b} is reasonably explained by the weaker hydrogen bond between the distal histidine and the oxygen atom of the ferryl oxo heme. These arguments suggest that the reactivity of compound **II** is regulated by Asn70 and His42 in a concerted way.

In conclusion, the elimination of the hydrogen bond between the N_δ-proton of His42 and Asn70 by mutations of Asn70 affects the active site structures of HRP in various oxidation and coordination states. The mutants favored the six-coordinate high-spin structure in the resting state. The pH titration of the Fe^{II}–His stretch clearly indicates the decreased basicity of His42 in the mutants. Thus far, it has been emphasized that the bond strength between heme iron and the sixth ligand (X) is affected by the distal His. However, we have demonstrated that mutations of Asn70, which is far from the heme and has no direct interactions with heme, notably affect the coordination and hydrogen bond strength of the Fe–X⋯His42 moiety. Thus, the importance of the concerted change of the hydrogen bonds of the heme distal side in the active site structure and enzymatic activity has been demonstrated.

Acknowledgment. We are grateful to Dr. Hiroshi Hori of Osaka University for his kind help in EPR measurements. This study was supported by a Grant-in-Aid for Scientific Research on Priority Area Molecular Biometallics from the Ministry of Education, Science, Culture and Sports, Japan, to T.K. (08249106) and to I.M. (08249107).

JA9625510

(38) The fact that there were no obvious frequency changes between pH 7 and pH 10 means the pK of the acid–base transition to be lower than that of native HRP. However, we could not observe the frequency shift in the pH range between 4 and 7 (data not shown). Therefore, the lower pK_a value does not rationalize the pH insensitivity of the $\nu_{\text{Fe=O}}$ frequency of the mutant compound **II**.